JOURNAL OF SEMICONDUCTOR TECHNOLOGY AND SCIENCE, VOL.16, NO.1, FEBRUARY, 2016
http://dx.doi.org/10.5573/JSTS.2016.16.1.106
ISSN(Print) 1598-1657
ISSN(Online) 2233-4866

Modeling of Electrolyte Thermal Noise in Electrolyte-Oxide-Semiconductor Field-Effect Transistors

Chan Hyeong Park and In-Young Chung*

Abstract—**Thermal noise generated in the electrolyte is modeled for the electrolyte-oxide-semiconductor field-effect transistors. Two noise sources contribute to output noise currents. One is the thermal noise generated in the bulk electrolyte region, and the other is the thermal noise from the double-layer region at the electrolyte-oxide interface. By employing two slightly-different equivalent circuits for two noise current sources, the power spectral density of output noise current is calculated. From the modeling and simulated results, the bulk electrolyte thermal noise dominates the double-layer thermal noise. Electrolyte thermal noise are computed for three different concentrations of NaCl electrolyte. The derived formulas give a good agreement with the published experimental data.**

Index Terms—**Thermal noise, electrolyte, oxide, semiconductor, field-effect, transistors**

I. INTRODUCTION

Nanobiosensors have become one of main players in the More-than-Moore ramifications of semiconductor industry. Nanobiosensors have distinctive advantages over the conventional biosensors including a very high sensitivity of femto Molar level in nanowire biosensors. Thus, there have been a lot of efforts being given to develop nanobiosensors [1-4]. Biosensors are categorized into three types: potentiometric, amperometric, and cantilever types [1]. Considering an integration compatibility with complementary-metal-oxide-semiconductor (CMOS) technology, the potentiometric biosensors have quite a natural characteristic because their structures are of a similar form as that of the conventional metal-oxide-semiconductor field-effect transistor (MOSFET). Already, a commercial DNA sequencing chip based on the potentiometric structure has been developed [4]. For these biosensors to be developed further into refined and reliable devices, electrical noise in them should be modeled and understood to shed light on overcoming the sensitivity limit of the nanobiosensors.

We are interested in the modeling of noise in the electrolyte-oxide-semiconductor field-effect transistors (EOSFETs) (see Fig. 1). They have been used as ion-sensitive FETs and pH-meters [1, 2]. Many papers have been published on the modeling of noise in EOSFETs [5-11]. One notable modeling approach was presented by Hassibi *et al.* in 2004 [5]. They modeled noise processes in the electrolyte-electrode system, and presented the formulas of noise from the double-layer region of the faradaic electrodes. However, they did not give a noise formula for the double-layer region of non-faradaic electrodes. In 2006, Jamal *et al.* extended the noise modeling into EOSFETs including a biomolecule-sensitive layer on top of the oxide, but did not cover thermal noise from the double-layer region, either [7]. Zheng *et al*. published a paper in 2009 demonstrating the increase of sensitivity by a factor of four by using the measurement of noise power spectral density (PSD) [9]. Very recently, Georgakopoulou *et al.* have modeled the noise behavior from the binding/unbinding of target molecules with receivers as well as the thermal noise in

Manuscript received Sep. 3, 2015; accepted Nov. 27, 2015
Department of Electronics and Communications Engineering, Kwangwoon University, Seoul 01897, Republic of Korea
E-mail : maybreez@kw.ac.kr

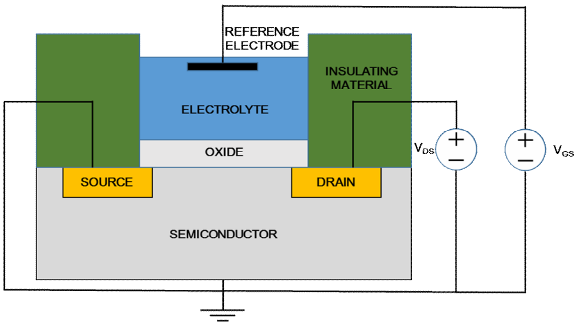

Fig. 1. Schematic diagram of an EOSFET.

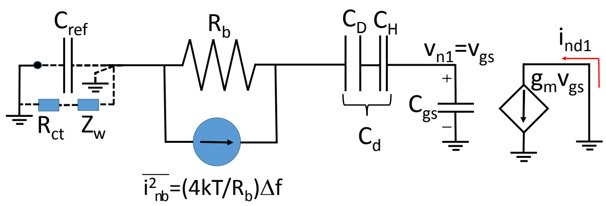

Fig. 2. Small-signal equivalent circuit of the EOSFET with the bulk thermal noise current source, i_{nb}.

the electrolyte, and showed an investigation on the screening effect to high-frequency noise [11]. In these previous studies, the noise coming from the double-layer region at the electrolyte-oxide interface has not yet been explicitly presented.

In this paper, we present two slightly-different equivalent circuit models for two independent thermal noise sources, one from the bulk electrolyte region and the other from the double-layer region at the electrolyte-oxide interface, and give an explicit derivation of electrolyte thermal noise formulas for EOSFETs. Until now, the thermal noise from the double-layer region has been ignored, nor treated well without explicit derivations or explanations. Thus, we present the explicit noise formulas from two regions, the bulk and the double-layer region, and show why the latter's contribution has been ignored up to now. The channel thermal noise in the FET and the low-frequency noise such as $1/f$ noise and generation-recombination noise in the oxide and in the semiconductor are not considered here. In this paper, we focus on the electrolyte thermal noise effect on the drain noise currents. Definitely, in the real-world EOSFET noise experiments, the channel thermal noise and the low-frequency noise from the oxide are present as well as the electrolyte thermal noise. One of the reasons why we did not insert these noise sources is that these noise sources are well treated in the previous literature, such as Ref. [7].

In Sec. II, the formulas of the PSD of output noise currents are derived due to two thermal noise sources. In Sec. III, the simulation results are given for 1:1 NaCl electrolyte. These simulation results are analyzed with three different electrolyte concentrations, and a qualitative comparison with the published experimental data is presented. Conclusions are summarized in Sec. IV.

II. MODELS

Fig. 2 shows a small-signal equivalent circuit that is commonly used in modeling of the impedance characteristics of the electrolyte-electrode system [12-14] except noise sources. Following Ref. [5], we consider two independent noise current sources whose power spectral densities are given as follows:

$$\overline{i_{nb}^2} = \left(4kT / R_b\right)\Delta f \qquad (1)$$

$$\overline{i_{nD}^2} = \left(4kT / R_D\right)\Delta f \qquad (2)$$

where $\overline{i_{nb}^2}$ is the mean square noise current in the bulk electrolyte, $\overline{i_{nD}^2}$ is the mean square noise current in the double-layer region, k is the Boltzmann constant, T the absolute temperature, R_b is the resistance of the bulk electrolyte, R_D is the "noise resistance" of the double-layer region which represents the random thermal movements of cations and anions inside the double-layer region, Δf is the frequency range where the noise measurement is done. Here, the ideal non-polarizable (faradaic) reference electrode is assumed such that the charge-transfer resistance R_{ct} and the Warburg impedance Z_w are negligible to zero ohms.

Noise calculation proceeds one at a time. First, let us calculate a noise voltage v_{n1} at the electrolyte-oxide interface due to i_{nb}. Second, v_{n2} due to i_{nD}.

1. Noise Voltage v_{n1} due to the Noise Current Source i_{nb}

From the small-signal equivalent circuit with the bulk thermal current noise source of Fig. 2, v_{n1} is derived and the mean square noise voltage $\overline{v_{n1}^2}$ from the bulk electrolyte can be written as:

$$\overline{v_{n1}^2}(f) = \frac{4kTR_b\left(\dfrac{C_d}{C_d + C_{gs}}\right)^2 \Delta f}{1+\left(\omega R_b\left(C_d \parallel C_{gs}\right)\right)^2} \qquad (3)$$

where ω (=$2\pi f$) is the angular frequency, C_d ($\equiv C_D \| C_H$) is the double-layer capacitance C_D in series with the Helmholtz capacitance C_H, and C_{gs} is the gate-to-source capacitance. Here, we use

$$C_D = \frac{\varepsilon_w A}{L_D}\cosh\left(\frac{q\psi_0}{2kT}\right) \cong \frac{\varepsilon_w A}{L_D} \qquad (4)$$

$$C_{gs} = \frac{2}{3}C_{ox} = \frac{2}{3}\frac{\varepsilon_{ox} A}{t_{ox}} \qquad (5)$$

$$C_H = \frac{\varepsilon_w A}{x_2} \qquad (6)$$

where $C_{gs} = (2/3)C_{ox}$ when the FET is in the saturation region, ε_w and ε_{ox} are the electrical permittivity of the water and the silicon dioxide, respectively, L_D is the Debye length of $\sqrt{\varepsilon_W kT/\left[2q^2 n_0\right]}$, $A=WL$, W, L are the width and length of the channel, n_+, n_- ($=n_0$) are the concentration of cations and anions, respectively, t_{ox} is the oxide thickness, and x_2 is the Stern layer thickness. An approximation in Eq. (4) holds when the electrostatic potential ψ_0 at the outer-Helmholtz plane is smaller than the thermal voltage kT/q.

Eq. (3) shows that the power spectral density $S_{v_{n1}}$ of the noise voltage v_{n1} has a low-frequency plateau level of $4kTR_b\left(C_d/\left(C_d + C_{gs}\right)\right)^2$ and its pole frequency is located at $f_{p1} = 1/\left[2\pi R_b\left(C_d \parallel C_{gs}\right)\right]$.

The point to note is that in calculating the effect of i_{nb} to the noise voltage v_{n1}, there is no resistance in the double-layer region, i.e. no R_D. The reason of why R_D should play no role in the transfer function from i_{nb} to v_{n1} in Fig. 2, is rather subtle. At the first sight, it seems natural to put R_D in parallel with C_D when we calculate the i_{nd1} from the i_{nb}. However, if we put a very small R_D in shunt with C_D, the small R_D would dominate the parallel admittance, distorting the whole v_{n1}. Thus, it is a right approach to omit the "noise resistance" R_D when the effect from the i_{nb} is considered. The transfer function is determined by the electrical double-layer structure, which is the series connection of the C_D, the C_H, and the C_{gs}.

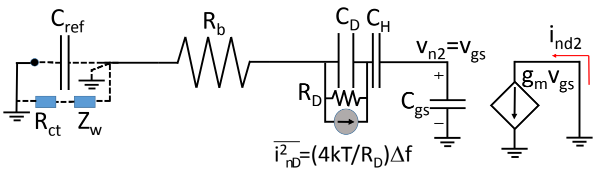

Fig. 3. Small-signal equivalent circuit of the EOSFET with the double-layer thermal noise current source, i_{nD}.

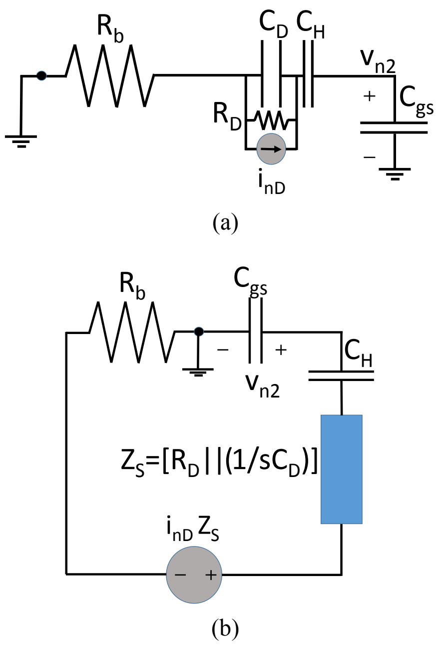

Fig. 4. (a) Noise voltage at the electrolyte-oxide interface due to the noise source i_{nD} in the double-layer region, (b) the Thévenin transformation to calculate the noise voltage v_{n2}.

2. Noise Voltage v_{n2} due to the Noise Current Source i_{nD}

Fig. 3 which is a newly-proposed model in this paper, considers the output noise current i_{nd2} from the noise current source i_{nD} inside the double-layer region.

Noise voltage v_{n2} at the electrolyte-oxide interface due to i_{nD} can be calculated by transforming the circuit of Fig. 4(a) into Fig. 4(b).

From the equivalent circuit of Fig. 4(b), we get

$$\overline{v_{n2}^2} = \frac{4kT\Delta f/R_D}{\omega^2 C_{gs}^{\ 2}}\left|\frac{\left(R_D \parallel \dfrac{1}{sC_D}\right)}{\left(R_D \parallel \dfrac{1}{sC_D}\right)+\left(\dfrac{1}{sC_{gs}}\right)+\left(\dfrac{1}{sC_H}\right)+R_b}\right|^2 \qquad (7)$$

Here, we also note that in calculating the effect of i_{nD} to the noise voltage v_{n2}, R_D should be included in the transfer function and this fact is rather subtle to grasp.

Combining Eqs. (3, 7), we finally arrive at the PSD of the noise voltage at the electrolyte-oxide interface to be

$$S_{v_n}(f) = S_{v_{n1}}(f) + S_{v_{n2}}(f) = \frac{4kTR_b\left(\frac{C_d}{C_d + C_{gs}}\right)^2}{1+\left(\omega R_b\left(C_d \parallel C_{gs}\right)\right)^2} + \frac{4kTR_D}{\left|\tau_2 s + \left(\tau_3 s + 1 + C_{gs}/C_H\right)\left(\tau_1 s + 1\right)\right|^2} \quad (8)$$

where the time constants are defined to be $\tau_1 \equiv R_D C_D$, $\tau_2 \equiv R_D C_{gs}$, $\tau_3 \equiv R_b C_{gs}$, respectively.

The PSD $S_{v_{n2}}$ of noise voltage v_{n2} has a low-frequency plateau level of $4kTR_D\left(C_H/\left(C_H + C_{gs}\right)\right)^2$, and its 3-dB bandwidth is estimated to be $f_{3-dB} \approx 1/\left[2\pi\left\{\left(C_H/\left(C_H + C_{gs}\right)\right)\left(\tau_3 + \tau_2\right) + \tau_1\right\}\right]$.

From Eq. (8), we predict that the noise PSD at the electrolyte-oxide interface is dominated by the bulk electrolyte thermal noise and the corner frequency is determined by $f_c = 1/\left[2\pi R_b\left(C_d \parallel C_{gs}\right)\right]$, because the double-layer noise resistance is much smaller than the bulk resistance, $R_D \ll R_b$. Thus, the PSD of the drain noise currents from the electrolyte thermal noise is modeled to be

$$S_{i_d}(f) \cong \frac{4kTR_b\left(\frac{C_d}{C_d + C_{gs}}\right)^2 g_m^2}{1+\left(\omega R_b\left(C_d \parallel C_{gs}\right)\right)^2} \quad (9)$$

where g_m is the transconductance of the EOSFET. In a real noise measurement, the channel thermal noise of the FET should be added to Eq. (8).

III. SIMULATION RESULTS

1. Simulation Results of the Derived Formulas

When the reference electrode area is much larger than the gate area of the EOSFET, the bulk resistance of the electrolyte can be approximated by the spreading resistance given by [7]

$$R_b \cong \frac{1}{\kappa}\sqrt{\frac{\pi}{WL}} \quad (10)$$

where κ is the electrolyte conductivity. To calculate κ, we use a simplified form of

$$\kappa \cong q\left(\mu_+ n_+ + \mu_- n_-\right) \quad (11)$$

neglecting the ion interaction effect, where q is the magnitude of electronic charge, μ_+, μ_- are the mobility of cations and anions, respectively. Table 1 shows the parameters that are used in the simulation. The mobility values of Na and Cl ions are typical values and the other parameters are adopted from Refs. [6, 7].

Although noise sources inside the double-layer region are distributed, and the concentration of cations and anions can change dramatically inside the diffuse region, we assume that the electrolyte-surface potential is rather small compared to the thermal voltage kT/q=26 mV at T=300 K, so that the noise resistance of the double-layer region is approximated to be

$$R_D \cong \frac{1}{\kappa}\frac{L_D}{A} \quad (12)$$

Table 2 shows the bulk resistance and the noise

Table 1. Simulation parameters for NaCl electrolyte

Temperature	300 K
Mobility of Na^+	5.19×10^{-4} cm^2/Vs
Mobility of Cl^-	7.91×10^{-4} cm^2/Vs
Electrolyte concentration	0.001, 0.01, 0.1 M
Dielectric constant of water	78.4
Dielectric constant of oxide	3.9
Oxide area	50 μm×50 μm
Oxide thickness	10 nm
Stern layer thickness	2 nm

Table 2. Calculated values of the EOSFET noise model elements with 50×50 μm² gate area

NaCl conc. (M)	κ (S/cm)	R_b (Ω)	R_D (Ω)	L_D (cm)	C_D/A (F/cm²)
0.001	1.26×10^{-4}	2.81×10^{6}	306	9.66×10^{-7}	7.19×10^{-6}
0.01	1.26×10^{-3}	2.81×10^{5}	9.68	3.05×10^{-7}	2.27×10^{-5}
0.1	1.26×10^{-2}	2.81×10^{4}	0.31	9.66×10^{-8}	7.19×10^{-5}

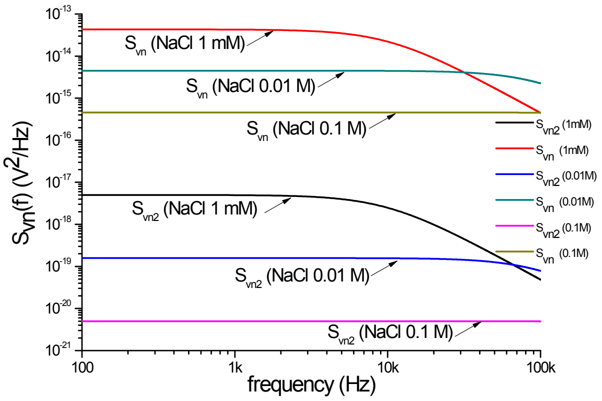

Fig. 5. Power spectral density of the noise voltage at the electrolyte-oxide interface of the EOSFET for three different NaCl electrolyte concentrations, 1mM, 0.01 M, and 0.1 M.

resistance of the diffuse region for three different electrolyte concentrations, 1 mM, 0.01 M, and 0.1 M.

Fig. 5 shows the calculated PSDs S_{v_n} and $S_{v_{n2}}$ from Eq. (8) of the noise voltage at the electrolyte-oxide interface of 1:1 NaCl electrolyte. Electrolyte concentrations are chosen to be 1 mM, 0.01 M, and 0.1 M, respectively. We can see that the noise voltage PSD is flat up to the corner frequency of $f_c = 1/\left[2\pi R_b \left(C_d \parallel C_{gs}\right)\right]$ and goes down with frequency minus squared. The corner frequencies are calculated to be 10.2 kHz, 100.1 kHz, and 994.3 kHz, respectively, and agree well with the simulated results of Fig. 5. As the electrolyte molar concentration increases, the bulk resistance of the electrolyte from Eq. (10) decreases as the electrolyte conductivity κ goes up according to Eq. (11). Since the low-frequency plateau level of S_{v_n} is proportional to R_b, we can see that why the plateau level goes down as the electrolyte molar concentration strengthens from 1mM to 0.01 M, and 0.1 M in Fig. 5.

We note that the bulk electrolyte thermal noise dominates the output noise, and the noise contribution from the double-layer region is negligible, which is consistent with the conventional models where the double-layer noise resistance R_D and its corresponding noise current source i_{nD} are not treated in the small-signal equivalent circuit model with noise sources [6, 7, 11, 15].

2. Comparison with Experimental Data

We compare the simulation results with the experimental data in a qualitative way. In Ref. [15], the Lorentzian spectrum of the electrolyte thermal noise was measured when the cell in a bath electrolyte was adhered on the open gate surface area. The low-frequency plateau level of 5×10^{-14} V²/Hz and the corner frequency of 63.7 kHz was measured. This measured Lorentzian spectrum is what our derived formula expects for the electrolyte thermal noise with R_b of 2.9 MΩ, C_d of infinity Farads, and C_{gs} being extended into (C_{gs}+C_M) where C_M is the membrane capacitance corresponding to the bulk electrolyte capacitance that has been ignored in our model (see Eq. (8)) . In the experiment of Ref. [15], when the neuron cell membrane adheres to the oxide surface, the effective bulk electrolyte capacitance becomes large because the width of the cleft which acts as a bulk electrolyte becomes very short of the order of 50 nm, with the C_M competing with the C_{gs} in magnitude. Thus, with the inclusion of the bulk capacitance effect into our presented model, the experimental data of Ref. [15] agree well the simulated results of our derived formulas of the electrolyte thermal noise.

IV. CONCLUSIONS

We modeled the electrolyte thermal noise in EOSFETs and presented the output noise formulas from noise sources in the bulk electrolyte and in the double-layer region.

We showed that the PSD of the noise voltage at the electrolyte-oxide surface is dominated by the bulk electrolyte thermal noise. The noise spectrum shows the Lorentzian form whose corner frequency increases as the electrolyte concentration does. The simulation results are expected to be used to estimate the limit of detection level of nanobiosensors.

ACKNOWLEDGMENTS

This work was supported by the Research Grant of

Kwangwoon University in 2013. This research was also supported by Basic Science Research Program through the National Research Foundation of Korea (NRF) funded by the Ministry of Education (NRF-2010-0023999).

REFERENCES

[1] M. A. Alam, *Principles of Electronic Nanobiosensors*, www.nanohub.org, 2013.

[2] P. Bergveld, “Thirty years of ISFETOLOGY: What happened in the past 30 years and what may happen in the next 30 years,” *Sens. Actuators B*, vol. 88, pp. 1-20, 2002.

[3] X. P. A. Gao, G. Zheng, and C. M. Lieber, “Subthreshold regime has the optimal sensitivity for rnanowire FET biosensors,” *Nano Lett.*, vol. 10, pp. 547-552, 2010.

[4] J. M. Rothberg *et al.*, “An integrated semiconductor device enabling non-optical genome sequencing,” *Nature*, vol. 475, pp. 348-352, 2011.

[5] A. Hassibi, R. Navid, R. W. Dutton, and T. H. Lee, “Comprehensive study of noise processes in electrode electrolyte interfaces,” *J. Appl. Phys.*, vol. 96, pp. 1074-1082, 2004.

[6] D. Landheer, G. Aers, W. R. McKinnon, M. J. Deen, and J. C. Ranuarez, “Model for the field effect from layers of biological macromolecules on the gates of metal-oxide-semiconductor transistors,” *J. Appl. Phys.*, vol. 98, pp. 044701-1-15, 2005.

[7] M. J. Deen, M. W. Shinwari, J. C. Ranuárez and D. Landheer, “Noise considerations in field-effect biosensors,” *J. Appl. Phys.*, vol. 100, pp. 074703-1-8, 2006.

[8] A. Hassibi, H. Vikalo, and A. Hajimiri, “On noise processes and limits of performance in biosensors,” *J. Appl. Phys.*, vol. 102, pp. 014909-1-12, 2007.

[9] G. Zheng, X. P. A. Gao, and C. M. Lieber, “Frequency domain detection of biomolecules using silicon nanowire biosensors,” *Nano Lett.*, vol. 10, pp. 3179-3183, 2010.

[10] J. Go, P. R. Nair, and M. A. Alam, “Theory of signal and noise in double-gated nanoscale electronic pH sensors,” *J. Appl. Phys.*, vol. 112, pp. 034516-1-10, 2012.

[11] K. Georgakopoulou, A. Birbas, and C. Spathis, “Modeling of fluctuation processes on the biochemically sensorial surface of silicon nanowire field-effect transistors,” *J. Appl. Phys.*, vol. 117, pp. 104505-1-8, 2015.

[12] J. O’M. Bockris, A. K. N. Reddy, and M. Gamboa-Aldeco, *Modern Electrochemistry: Fundamentals of Electrodics*, vol. 2A, 2nd ed. 2000, Kluwer Academic.

[13] E. Gileadi, *Electrode Kinetics for Chemists, Chemical Engineers, and Material Scientist*, 1993, Wiley-VCH.

[14] A. J. Bard and L. J. Faulkner, *Electrochemical Methods: Fundamentals and Applications*, 2nd ed. 2001, Wiley.

[15] M. Voelker and P. Fromherz, “Nyquist noise of cell adhesion detected in a neuron-silicon transistor,” *Phys. Rev. Lett.*, vol. 96, pp. 228102-1-4, 2006.

Chan Hyeong Park received the B.S., M.S., and Ph.D. degrees in electronics engineering from Seoul National University, Seoul, Korea, in 1992, 1994, and 2000, respectively. From 2000 to 2003, and from 2009 to 2012 he was a Visiting Scientist and a Visiting Professor, respectively with the Research Laboratory of Electronics, Massachusetts Institute of Technology (MIT), Cambridge. Since 2003, he has been with Kwangwoon University, Seoul, where he is currently a Full Professor with the Department of Electronics and Communications Engineering. His current research interests include the modeling of semiconductor devices and biosensors.

In-Young Chung received the B.S., M.S., and Ph.D. degrees in electronics engineering from Seoul National University, Seoul, Korea, in 1994, 1996, and 2000, respectively. He worked at Samsung Electronics from 2000 to 2004, where he designed DRAM circuits. He joined Gyeongsang National University as a faculty member in 2004. Since 2008, he has been with Kwangwoon University, Seoul, where he is currently a Full Professor with the Department of Electronics and Communications Engineering. He was a visiting scholar at University of California at Santa Barbara in 2014. His current research interests include the simulation and modeling of nano-devices and biosensors.